Physics Faculty Research & Creative Works   Physics

01 Jan 1983

Homogeneous Nucleation Of Toluene

John L. Schmitt
Missouri University of Science and Technology, jschmitt@mst.edu

R. A. Zalabsky

G. W. Adams

Recommended Citation

Homogeneous nucleation of toluene ⊘

J. L. Schmitt; R. A. Zalabsky; G. W. Adams

Check for updates

View Online

Export Citation

CrossMark

17 July 2023 15:44:52

Homogeneous nucleation of toluene

J. L. Schmitt, R. A. Zalabsky, and G. W. Adams

Physics Department and Graduate Center for Cloud Physics Research, University of Missouri-Rolla, Rolla, Missouri 65401

The authors have used a fast expansion chamber to measure the homogeneous nucleation rate of toluene as a function of temperature and supersaturation. The measured nucleation rate ranges from 10^2 to 10^5 drops/cm^3 s over a temperature range of 215–267 K. The measurements are compared with the "classical" nucleation theory and with the RKC theory. The inclusion of the RKC replacement factor brings the data into good agreement with theory using physically realistic values of the surface tension and the sticking coefficient. An empirical curve fit to the data is presented as well as a full listing of the thermodynamic constants used for the calculations.

I. INTRODUCTION

The vapor to liquid phase transition which takes place in a metastable, supersaturated vapor in the absence of catalytic nucleation sites is called homogeneous nucleation. The apparent physical simplicity of the homogeneous nucleation process makes a comprehensive understanding of its nature essential for unraveling the more complicated heteromolecular and heterogeneous nucleation processes.

The classical nucleation theory resulting from the work of Volmer,[1] Becker and Doring,[2] and Zeldovitich[3,4] is a superposition of equilibrium statistical mechanics and unimolecular reaction kinetics. The height of the free energy barrier to nucleation is estimated using the thermodynamic parameters appropriate for macroscopic liquid droplets. The need to modify the classical theory to include the effects of the translational and rotational energy in the critical clusters has long been recognized but an exact formulation a matter of controversy. Early formulations of the replacement free energy by Lothe and Pound[5] predicted that the nucleation rate obtained from the classical theory was too low by a factor of 10^{17}. A formulation of the replacement factor by Reiss, Katz, and Cohen,[6] and Reiss[7] (the RKC theory) indicates that, to be consistent with the liquid drop model of the capillarity approximation, the correction term should lie in the 10^3 to 10^6 range. As shown below a replacement factor of the order of 10^6 brings theory into good agreement with our toluene data.

The classical and modified classical (via the replacement factor) theories offer ease of evaluation by using a small number of readily available macroscopic parameters and provide useful standards for comparison of differing experimental techniques and the nucleating behavior of different substances. Fundamentally, however, the physics of the nucleation process must be understood on a molecular level. Although no complete microscopic theory is yet available for a variety of substances with widely differing molecular properties, significant progress has been made in this direction. Molecular dynamical and Monte Carlo approaches have been applied to estimate the physical properties of small clusters. Hale and Plummer[8] developed a molecular model for the homogeneous nucleation of water. Molecular approaches have yielded free energies of formation (Lee, Barker, and Abraham,[9] Garcia and Torroja[10]), effective surface tensions and surface free energies (Hale and Ward[11]) and microcrystalline free energies (Hoare, Pal, and Wegener[12]).

Experimental measurements of nucleation rates have been carried out with shock tubes,[13] supersonic nozzles,[14] and atomic beam apparatus[15] which provide insight into the nucleation process on a molecular level under nonequilibrium conditions. Diffusion and expansion cloud chambers, however, measure nucleation rates under well defined equilibrium conditions and provide data which can be directly compared to theory. A number of workers have obtained excellent results using diffusion cloud chambers for a variety of substances (Katz,[16-19] Reiss and Heist,[20] Heist, Colling, and Dupuis[21]). Previously measurements of nucleation rate using diffusion cloud chambers have been confined to the supersaturation rate corresponding to the onset of the nucleation process. However, workers are now using the diffusion chamber to measure nucleation rates from 10^{-2} to 10^2 drops/cm^3 s (Heist and Maguluri[22]). Expansion cloud chambers used in this laboratory have produced extensive data sets for water (Miller, Anderson, Kassner, and Hagen,[23] Miller[24]), ethanol (Schmitt, Adams, and Zalabsky[25]), toluene (this article), and nonane (Adams, Schmitt, and Zalabsky, to be published) with nucleation rates ranging from 10^2 to 10^5 drops/cm^3 s. Wagner and Strey[26] have nucleated 10^5 to 10^9 drops/cm^3 s in several substances. The expansion cloud chamber provides measurements of nucleation rate that complement those of the diffusion chamber.

This article presents our measurements of the homogeneous nucleation of toluene. An extensive new data set is presented and compared with the classical and a modified classical nucleation theory. Finally, an empirical equation is presented which allows calculation of the nucleation rate over the range of our measurements.

II. THE EXPANSION CHAMBER-EXPERIMENTAL PROCEDURE

The experimental results reported here were obtained with a precision expansion chamber. A detailed description of this chamber is given by Schmitt.[27] A brief description of the chamber and the details of its experimental operation is found in Schmitt, Adams, and Zalab-

sky.[25] The toluene experimental measurements reported here were performed in the chamber and manner described in these two references. In addition, the article by Schmitt, Kassner, and Podzimek[28] gives an extensive review of the design and operation of an expansion chamber for aerosol characterization.

III. CALCULATION OF THE TEMPERATURE AND SUPERSATURATION RATIO

The thermodynamic calculations are made assuming that the sensitive volume of our chamber remains dry adiabatic while nucleation is taking place. The validity of this assumption has been well demonstrated (see references for Sec. II). However, we wish to emphasize that since the expansions are sufficiently fast and the total drop counts sufficiently low, molecular heat transport and vapor depletion have a negligible effect on the thermodynamics of the sensitive volume. The nucleation and droplet growth processes are almost completely decoupled.

The thermodynamic calculations and estimates of temperature and supersaturation errors have been discussed extensively elsewhere (Schmitt, Adams, and Zalabsky[25]) and only the following brief review is included here. The temperature pressure relationship for a dry adiabatic expansion of a homogeneous substance is given by the standard equation

$$d \ln T = \frac{P(\partial \nu_m / \partial T)_{Pd} \ln P}{C_{pm}} , \qquad (1)$$

where ν_m is the molar volume of the gas mixture, P the total pressure, and C_{pm} the heat capacity of the gas mixture. The calculations were performed treating the gases (argon and toluene) as a mixture of real interacting gases. The partial derivative was evaluated using a virial equation of state truncated at the second virial coefficient and the heat capacities were corrected for real gas effects. For each preexpansion temperature T_0, Eq. (1) was integrated to find temperature and supersaturation ratio S as a function of P for a set of preexpansion pressures P_0. The calculated values were then curve fitted to obtain, for given T_0, P_0, T vs P and S vs P, relations of the form

$$T(P, P_0; T_0) = A_1(P_0) + A_2(P_0)P + A_3(P_0)P^2 + A_4(P_0)P^3 \quad (2a)$$

and

$$S(P, P_0; T_0) = B_1(P_0) + B_2(P_0)P + B_3(P_0)P^2 + B_4(P_0)P^3 . \quad (2b)$$

The $A_i(P_0)$ and $B_i(P_0)$ functions were then curve fit as a function of P_0 for each preexpansion temperature (T_0) to yield T vs P and S vs P relationships as follows:

$$T(P, P_0; T_0) = \sum_{i=1}^{4} \sum_{j=1}^{4} T_{ij}^{T_0} P_0^{j-1} P^{i-1} \qquad (3a)$$

and

$$S(P, P_0; T_0) = \sum_{i=1}^{4} \sum_{j=1}^{4} S_{ij}^{T_0} P_0^{j-1} P^{i-1} , \qquad (3b)$$

where, e. g., the i, j element of the temperature matrix is the jth expansion coefficient of the ith function in Eq. (2a). The temperature and supersaturation matrices allow the temperature and supersaturation ratios to be

rigorously calculated over the entire range of initial and final pressures which occur in the measurements. A separate pair of matrices was generated for each preexpansion temperature T_0. The thermodynamic parameters used in the temperature and supersaturation matrices are listed in the Appendix along with thermodynamic data used in subsequent calculations.

There are a number of sources of error in the temperature and supersaturation ratio: (1) uncertainties in the thermodynamic parameters, (2) pressure measurement accuracy, and (3) a small temperature gradient between the surface of the liquid pool and the upper glass plate. Our best estimate of the total error in the supersaturation ratio lies in the 1%–2% range with a much smaller temperature error.[25]

IV. HOMOGENEOUS NUCLEATION RATES FOR TOLUENE-DATA ANALYSIS

The toluene measurements are shown in Fig. 1 with the various data groups labeled according to their preexpansion temperatures T_0. The data was curve fit with two different functional forms of the nucleation rate equation

$$J_c(S, T) = S^2 \exp[A(T) + B(T)/(\ln S)^2] \qquad (4a)$$

and

$$J_H(S, T) = \Gamma_{rep}(S, T)S^2 \exp[A(T) + B(T)/(\ln S)^2] . \qquad (4b)$$

The term $\Gamma_{rep}(S, T)$ is a replacement factor formulated by Reiss, Katz, and Cohen,[6] and Reiss[7] and is given explicitly by (see the Appendix)

$$\Gamma_{rep}(S, T) = \beta \left[\frac{-2B(T)}{(\ln S)^3} \right]^{1/2} \frac{Td(T)}{P_e(T)S} . \qquad (5)$$

$A(T)$ and $B(T)$ are functions of the temperature only and are expanded in polynomial form. $d(T)$ is the bulk liquid density, $P_e(T)$ the saturation vapor pressure, and β is a constant given by

$$\beta = \frac{R}{M_w} \left(\frac{12}{\pi} \right)^{3/2} , \qquad (6)$$

where R is the gas constant and M_w the molecular weight. The form of Eq. (4a) facilitates comparison with the classical theory and has been used successfully by Miller[24] and Schmitt, Adams, and Zalabsky[25] to fit data sets for water and ethanol. The reason for fitting the toluene data with both Eqs. (4a) and (4b) will become apparent below.

The coefficients in the $A(T)$ and $B(T)$ polynomial functions were determined by using a nonlinear least squares search procedure which minimized the quantity

$$\chi^2 = \sum_{i=1}^{N} \frac{1}{N_i^m} (N_i^m - N_i^c)^2 , \qquad (7)$$

where the N^m are the measured drop concentrations and N^c those calculated by integrating Eqs. (4a) or (4b) over the nucleation pulses, i. e.,

$$N_i^c = \int_{-t_0}^{t_0} J[S(t), T(t)] dt , \qquad (8)$$

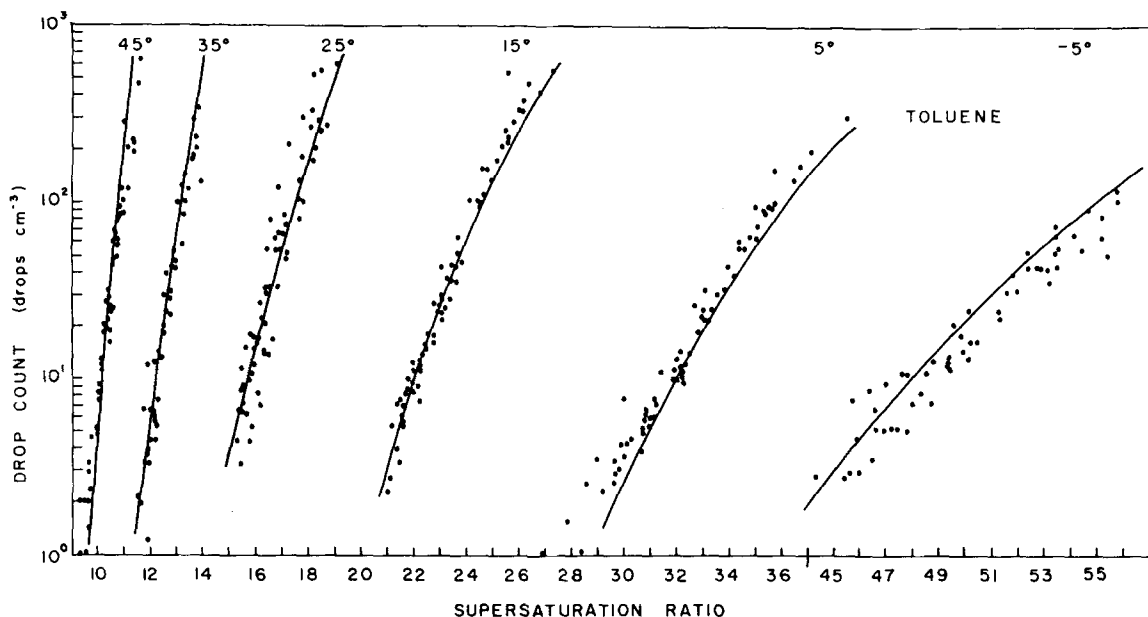where J is the nucleation rate in drops/cm^3 s. For each

FIG. 1. Measurements of the drops/cm^3 (not per s) nucleated in toluene as a function of supersaturation ratio. The solid curves show the empirical fit to the data (see Sec. VI of the text). The preexpansion temperature of each data group is near the top of the graph. The solid curves are also the prediction of the RKC theory if the physically "real" surface tension and sticking coefficient shown in Figs. 4 and 5 are used.

chamber expansion the peak (minimum) pressure is measured directly. The pressure vs time profile in the vicinity of the minimum pressure is checked at regular intervals and does not change significantly. (See the Appendix for the form of the pressure vs time profile.) The integration limits over the pulse are initially chosen as 0. 005 s and then increased until no significant changes were seen in the $A(T)$ and $B(T)$ functions. The $A(T)$ and $B(T)$ functions obtained using Eq. (4b) are listed in Sec. VI. Equation (4b) predicts the measured drop counts to within 50% for all data. It is valid in the temperature range 215–267 K. It should not, however, be extrapolated outside of this temperature range as it has a nonphysical turning point around 290 K. The solid lines in Fig. 1 were calculated using the curve fit with the $A(T)$ and $B(T)$ functions obtained with Eq. (4b).

V. COMPARISON WITH THEORY

The comparison of the data with theory is readily done by writing the classical theory in the form

$$J_{class}(S, T) = S^2 \exp[A_c(T) + B_c(T)/(\ln S)^2] , \quad (4a)$$

where

$$A_c(T) = \ln\left[\left(\frac{\alpha}{d}\right)(2M_w N_0^3 / \pi)^{1/2}\left(\frac{P_e}{RT}\right)^2\right] \quad (9)$$

and

$$B_e(T) = -\frac{16N_0}{3} \left(\frac{M_w}{d}\right)^2\left(\frac{\sigma}{RT}\right)^3 , \quad (10)$$

where α is the sticking coefficient, σ the bulk surface tension, and N_0 Avogadro's number. $A_c(T)$ and $B_c(T)$ depend on temperature only and correspond directly to the $A(T)$ and $B(T)$ functions in Eqs. (4a) and (4b).

Figure 2 shows the drop counts calculated using the classical theory and the classical theory multiplied by the replacement factor in Eq. (4b) (RKC theory). The values of the surface tension, liquid density, and saturation vapor pressure used in the calculations are listed in the Appendix. The sticking coefficient was set equal to unity for the calculations shown in Fig. 2. The classical theory shows marked deviations from the data, increasingly so at lower temperatures. Inclusion of the replacement factor brings the theory into considerably better agreement with the data. Note that in Fig. 2 the solid lines are the classical theory and the dashed lines the RKC theory. The classical theory predictions must be multiplied by the factors (e. g., 10^5, 10^4) shown near the bottom of the graph to achieve the fit shown in Fig. 2. The RKC theory predictions must be multiplied by 10^{-1} (all curves) to achieve the shown fit. Thus Eq. (4b) was chosen as the more appropriate functional form to fit the data. Curve fits to the data were used to predict critical supersaturation, surface tension, and sticking coefficient.

The critical supersaturation ratios predicted by the curve fit [Eq. (4b)] to our data are shown in Fig. 3 along with the diffusion chamber data of Katz, Scoppa, Kumar, and Mirabel.[18] The deviations of our data from the classical theory and Katz' data increase with decreasing temperature. However, our measurements are in the range 10^2–10^5 drops/cm^3 s and a two order of magnitude extrapolation is necessary (via the curve fit) to predict the critical curve.

The curve fits were used to calculate the sticking coefficients and surface tensions required for the classical and RKC theories to be in exact agreement with the measurements. The surface tensions inferred from the data
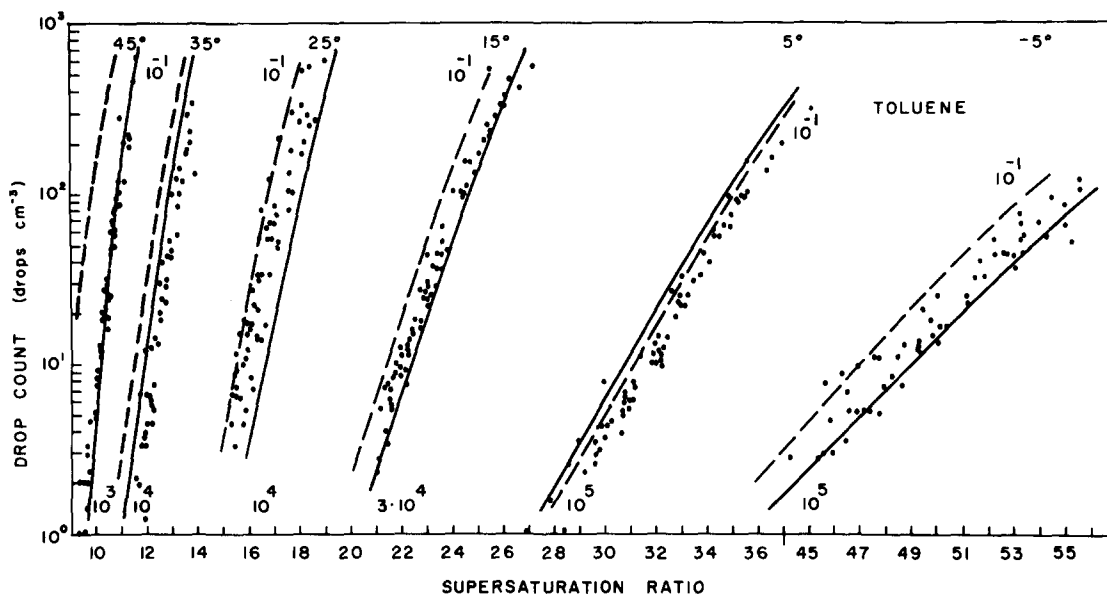
FIG. 2. A comparison of theory with the measured nucleation of toluene. The solid curves show the predictions of the classical theory with a sticking coefficient of unity and the bulk surface tension. The classical theory must be multiplied by the indicated factors at the bottom of the grap (e.g., 10^5) to obtain the shown agreement with the data. The dashed curves are the predictions of of the RKC theory with a sticking coefficient of unity and the bulk surface tension. The RKC theory must be multiplied by a constant factor of 10^{-1} (top of graph) to obtain the shown agreement with the data.

are shown in Fig. 4 along with the measured bulk values. The sticking coefficients are shown in Fig. 5. The surface tensions and sticking coefficients obtained without the replacement factor [Eq. (4a)] are physically nonrealistic. In particular the sticking coefficient ranges from 10^{-4} to 10^2 which is clearly physically meaningless. In-

clusion of the replacement factor [Eq. (4b)] results in physically realistic sticking coefficients (e. g., values ranging from 0. 002 to 1 have been measured for water[29]) and surface tensions which lie only a few percent below the bulk value and have approximately the same linearily decreasing temperature dependency as bulk liquid values.

The physically unrealistic behavior of the surface tension and sticking coefficient when the classical theory form [Eq. (4a)] is used clearly is a reflection of a missing temperature and supersaturation dependency. The re-
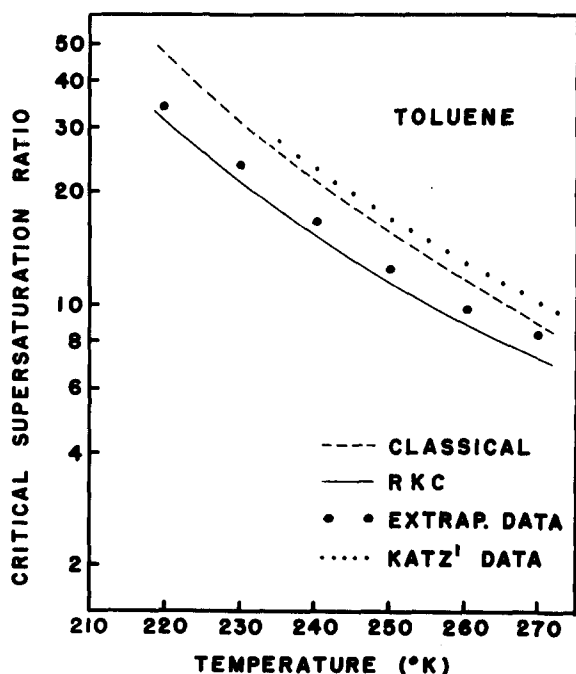

FIG. 3. The critical supersaturation as a function of temperature for toluene, as measured by Katz, predicted by the classical theory, predicted by the RKC theory discussed in this article and predicted by extrapolation of our measurements.
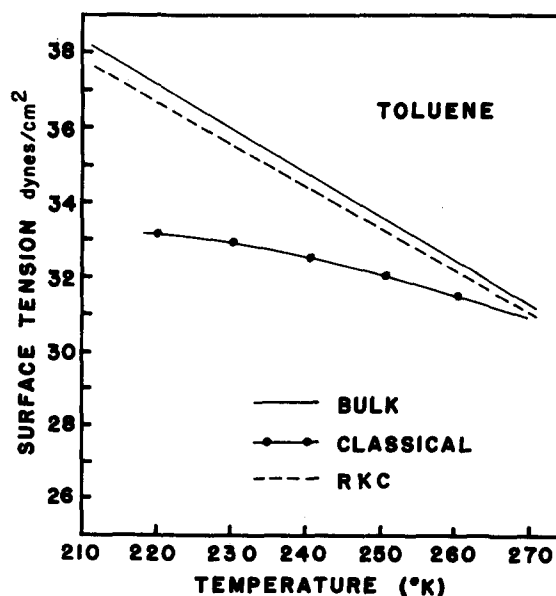

FIG. 4. The surface tension of toluene as a function of temperature as measured and predicted (see the text).
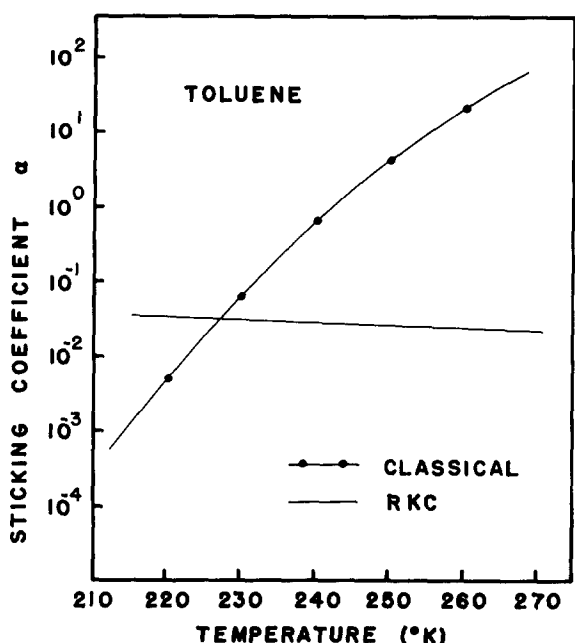
FIG. 5. The sticking coefficient of toluene as predicted by the classical and RKC theories (see the text).

placement factor used corresponding to the upper limit estimated for Γ_{rep} by Reiss, Katz, and Cohen,[6] and Reiss[7] is one possible choice but not necessarily the only one. The capillarity approximation is intrinsically in error even when microscopic corrections are applied to the parameters (liquid density, surface tension, and sticking coefficient). It is possible that errors in the free energy barrier due to capillarity may be compensated for with an incorrect replacement factor. The present analysis suggests, however, that the critical clusters of toluene may have properties very close to those of the bulk liquid and indicates that the magnitude of the re-placement factor used is essentially correct. The size of the critical clusters may be estimated from[24]

$$n^* = \frac{-2B(T)}{(\ln S)^3} , \tag{11}$$

where $B(T)$ is obtained from the data via the curve fit. The toluene critical cluster sizes over the temperature and supersaturation range of the data vary from about 20 to 50 molecules. According to recent calculations by Sinanoglu[30] nonpolar clusters of molecules such as ben-zene and toluene have a surface tension some 5% lower than that of the bulk liquid values for clusters contain-ing less than ten molecules. These calculations support the results of our analysis, i.e., the toluene clusters are of sufficient size and/or molecular character that their properties may be well approximated by those of the bulk liquid.

VI. CONCLUSIONS

We have measured homogeneous nucleation rates for toluene from 10^2 to 10^5 drops/cm^3 s over a temperature range of 215–267 K. The data is reproduced by the empirical nucleation rate equation

$$J_H(S, T) = \Gamma_{rep}(S, T)S^2 \exp[A(T) + B(T)/(\ln S)^2], \tag{4b}$$

where

$$\Gamma_{rep}(S, T) = \beta\left[\frac{-2B(T)}{(\ln S)^3}\right]^{1/2} \frac{Td(T)}{P_e(T)S} \tag{5}$$

and

$$\beta = \frac{R}{M_w}\left(\frac{12}{\pi}\right)^{3/2} . \tag{6}$$

Here $A(T) = -42.403\,811\,874 + 0.578\,651\,0112 \times T$

$$-0.873\,937\,7184 \times 10^{-3}T^2$$

and

$B(T) = -0.105\,628\,887\,672 \times 10^5 + 72.564\,861\,1211 \times T$

$$-0.128\,053\,719\,442 \times T^2 .$$

The equations for the thermodynamic parameters are given in the Appendix.

Toluene nucleation rates are not predicted well by the classical nucleation theory which departs increasingly with decreasing temperatures, and surface tensions and sticking coefficients inferred from the classical theory functional fit to the data are not physically correct, in-dicating some missing temperature and supersaturation dependence. However, inclusion of the upper limit of the replacement factor formulated by Reiss, Katz, and Cohen,[6] and Reiss,[7] (RKC theory) although not the only possible correction, produces T and S dependencies which correctly predict the measured nucleation rates and result in surface tension and sticking coefficients which are physically reasonable. Our analysis suggests that the toluene critical clusters in this work by virtue of their size and/or molecular nature may have physical properties close to those of the bulk liquid.

ACKNOWLEDGMENTS

APPENDIX

Table I lists the various thermodynamic parameters used in the reduction of the data. For those investiga-tors who wish to rereduce the measurements we have made a list of the approximately 375 measurements (Fig. 1) and it is available upon application to the authors. In the list are the initial pressure (preexpansion), the minimum pressure (peak), the calculated expanded tem-perature, the calculated peak supersaturation ratio, the measured drop count, and the drop count calculated from the empirical fit to Eq. (4b). The pressure pulse for all data sets is given explicitly by

$$P(t) = P_{min} + 1.143t + (3.3945 \times 10^5)t^2 ,$$

where 0.01 s$> t > -0.01$ s (t is measured from the peak of the pulse), t is in s, and P is in mmHg. Note that this pulse shape is a correction to that given in Refs. 25 and 27.

TABLE I. Thermodynamic parameters.

Ideal gas heat capacities[a] (ergs/mol K)

$C_{p1} = 4.186 \times 10^7 \, (-4.43622 \times 10^{-2} + 8.58873 \times 10^{-2} T - 7.81856 \times 10^{-6} T^2)$[b]

$C_{p2} = 2.0776 \times 10^8$ [c]

Saturation vapor pressure-toluene (dyn/cm^2)

$P_e(T) = 9997.532415 \, e^x$

where $x = 30.629588 - 6289.3763/T - 0.035932503T + 0.28297458 \times 10^{-4} T^2$[d]

Second virial coefficients (cm^3/mol)

$B_1(T) = R \, T_c/P_c \, [f^{(0)}(T_r) + \omega f^{(1)}(T_r)]$,[e]

where $T_r = T/T_c$, $T_c = 594.025$ and $\omega = 0.2607$

$f^{(0)}(T_r) = 0.1445 - 0.330/T_r - 0.1385/T_r^2 - 0.0121/T_r^3$

$f^{(1)}(T_r) = 0.073 + 0.46/T_r - 0.50/T_r^2 - 0.097/T_r^3 - 0.0073/T_r^8$

$B_2(T) = -1150.935 + 20.7692T - 0.1678223T^2 + 0.7125312 \times 10^{-3} T^3 - 0.1541841 \times 10^{-5} T^4 + 0.1341542 \times 10^{-8} T^5$[f]

Liquid density (gm/cm^3)

$d = 0.96367 + 0.10735 \times 10^{-2} T - 0.87898 \times 10^{-5} T^2 + 0.17846 \times 10^{-7} T^3 - 0.14326 \times 10^{-10} T^4$[g]

Surface tension (dyn/cm^2)

$= 30.90 - 0.1189(T - 273.15)$[h]

[a]Subscript 1 refers to the toluene and 2 to the argon.
[b]Thermophysical Properties of Matter (IFI/Plenum, New York, 1970), Vol. 6. Specific Heat, Nonmetallic Liquid and Gases.
[c]Thermodynamics Research Center, Selected Values of Properties of Hydrocarbons and Related Compounds (Texas A&M University, College Station, Texas, 1965).
[d]Buford Smith, Dept. of Chemical Engineering, Washington, University, St. Louis, Missouri (private communication).
[e]K. S. Pitzer and R. F. Curl, J. Am. Chem. Soc. 79, 2369 (1957).
[f]From fit of points in The Thermodynamic Properties of Argon from The Triple Point to 100 K at pressures to 1000 Atmospheres, Natl. Bur. Stand. (U.S. GPO, Washington, D.C., 1969).
[g]J. L. Hales and R. Townsends, J. Chem. Theromdyn. 4, 763 (1972).
[h]J. L. Jasper, J. Phys. Chem. Ref. Data 1, 841 (1972).

The replacement factor [Eq. (5)] is found as follows. Reiss, Katz, and Cohen,[6] and Reiss[7] give an upper limit for the replacement factor in the form

$$\Gamma_{rep}(S, T) \leq (n^*)^{1/2} \left(\frac{\nu_g}{\nu_l}\right)\left(\frac{12}{\pi}\right)^{3/2} \,.$$

The number of molecules n^* in a critical cluster is given by

$$n^* = -\frac{2B(T)}{(\ln S)^3} \,,$$

where $B(T)$ is obtained from the curve fit or evaluated

from theory. ν_g is the volume of a molecule in the gas phase and is given by

$$\nu_g = \frac{kT}{P_e(T)S} \,.$$

ν_l is the volume of a molecule in the liquid phase and is given by

$$\nu_l = \frac{M_w}{N_0 d(T)} \,.$$

Substitution into the initial equation here gives Eq. (5).

[1]M. Volmer, Z. Phys. Chem. 25, 555 (1929).
[2]R. Becker and W. Doring, Ann. Phys. 24, 719 (1935).
[3]J. B. Zeldovitch, J. Exp. Theor. Phys. 12, 525 (1942).
[4]J. B. Zeldovitch, Acta. Phys. Chem. USSR 18, 1 (1943).
[5]J. Lothe and G. M. Pound, J. Chem. Phys. 36, 2082 (1962).
[6]H. Reiss, J. L. Katz, and E. R. Cohen, J. Chem. Phys. 48, 5553 (1968).
[7]H. Reiss, Nucleation Phenomena, edited by A. C. Zettlemeyer (Elsevier, New York, 1977), pp. 1–66.
[8]B. N. Hale and P. L. M. Plummer, J. Chem. Phys. 61, 4012 (1974).
[9]J. K. Lee, J. A. Barker, and F. F. Abraham, J. Chem. Phys. 58, 3166 (1973).
[10]N. G. Garcia and J. M. Torrojz, Phys. Rev. Lett. 47, 186 (1981).
[11]B. N. Hale and R. C. Ward, J. Stat. Phys. 28, 487 (1982).
[12]M. R. Hoare, P. Pal, and P. P. Wegener, J. Colloid Interface Sci. 75, 126 (1980).
[13]F. Peters, J. Chem. Phys. 77, 4788 (1982).
[14]P. P. Wegener and B. J. C. Wu, Nucleation Phenomena, edited by A. C. Zettlemeyer (Elsevier, New York, 1977), pp. 325–417.
[15]A. W. Castleman, Jr., Kinetics of Ion–Molecule Reaction, edited by P. Ausloos (Plenum, New York, 1979), pp. 295–321.
[16]J. Katz and B. J. Ostermier, J. Chem. Phys. 47, 478 (1967).
[17]J. L. Katz, J. Chem. Phys. 52, 4733 (1970).
[18]J. L. Katz, C. J. Scoppa, N. G. Kumar, and P. Mirabel, J. Chem. Phys. 62, 448 (1975).
[19]J. L. Katz, P. Mirabel, and C. J. Scoppa II, J. Chem. Phys. 65, 382 (1976).
[20]R. Heist and H. Reiss, J. Chem. Phys. 59, 665 (1973).
[21]R. H. Heist, K. M. Colling, and C. S. Dupuis, J. Chem. Phys. 65, 5147 (1976).
[22]R. H. Heist and S. Maguluri, 56th Colloid and Surface Science Symposium, Blacksburg, Virginia, June 13–16, 1982.
[23]R. Miller, R. Andrrson, J. L. Kassner, Jr., and D. Hagen, J. Chem. Phys. 78, 3204 (1983).
[24]R. C. Miller, Ph.D. dissertation, University of Missouri, Rolla, Rolla, Missouri, 1976.
[25]J. L. Schmitt, G. W. Adams, and R. A. Zalabsky, J. Chem. Phys. 77, 2089 (1982).
[26]P. E. Wagner and R. Strey, J. Phys. Chem. 85, 2694 (1981).
[27]J. L. Schmitt, Rev. Sci. Instrum. 52, 1749 (1981).
[28]J. L. Schmitt, J. L. Kassner, Jr., and J. Podzimek, J. Aerosol Sci. 13, 373 (1982).
[29]A. F. Mills and R. A. Seban, Int. J. Heat Mass Transfer. 10, 1815 (1967).
[30]O. Sinanoglu, J. Chem. Phys. 75, 463 (1981).